AIAA JOURNAL
Vol. 30, No. 2, February 1992

Modeling Ideally Expanded Supersonic Turbulent Jet Flows with Nonpremixed H_2-Air Combustion

R. Villasenor*
Vanderbilt University, Nashville, Tennessee 37235
J.-Y. Chen†
Sandia National Laboratories, Livermore, California 94550
and
R. W. Pitz‡
Vanderbilt University, Nashville, Tennessee 37235

A prediction model for a turbulent axisymmetric diffusion flame with equilibrium and nonequilibrium hydrogen-air kinetics is presented for supersonic jet flows. For the first time, turbulence-chemistry interactions are included in a supersonic combustion model. In the finite rate chemistry analysis, the fast shuffle reactions in the H_2-air reaction system are assumed to be in partial equilibrium and three-body recombination reactions are treated kinetically. The turbulence model consists of the Navier-Stokes equations in Favre-averaged form with a modified two-equation turbulence closure adapted for supersonic flows. The model uses probability density functions to describe fluctuations in both the mixture fraction and the reaction progress variable. Other relevant features of the supersonic code include a local convective Mach number that quantifies the compressibility effects and a thermodynamic table technique that speeds up the numerical computation. The model predictions are compared to probe measurements in a supersonic H_2-air jet flame by Beach. Comparison of the mixture fraction deduced from Beach's data to the model results indicates that the model predicts the turbulent mixing reasonably well. Predictions of the major species concentrations are nearly identical for the equilibrium and partial equilibrium models. The partial equilibrium model predicts substantial superequilibrium of the minor species and more closely predicts Beach's data than an earlier chemistry model based on eddy breakup.

Nomenclature

C_D^0, C_g = turbulence model constants
f = mixture fraction
f_{cc} = correction factor
g = variance of mixture fraction
k = turbulent kinetic energy
M_c = convective Mach number
p = variance of progress variable
$\tilde{q}$ = progress variable
r = radial coordinate
Sc = Schmidt number
$\tilde{S}_q$ = source term
$\tilde{u}$ = longitudinal velocity component
$\tilde{v}$ = radial velocity component
x = longitudinal coordinate
γ = specific heat ratio
ϵ = turbulence dissipation rate
μ = dynamic viscosity
$\tilde{\rho}$ = density
σ = Prandtl-Schmidt number
τ = time scale ratio
$\tilde{\chi}_2$ = second mixing term of q equation

Received Feb. 19, 1990; revision received July 16, 1991; accepted for publication Aug. 1, 1991.

*Graduate Student, Mechanical Engineering. Member AIAA.
†Member of Technical Staff. Member AIAA.
‡Associate Professor, Mechanical Engineering. Senior Member AIAA.

Introduction

A VITAL part of the effort to develop advanced propulsion systems capable of sustaining hypersonic flight within the atmosphere is the ability for theoretical prediction of flow properties in scramjet combustors where hydrogen is injected and burned in a supersonic airstream. For complete generality, the prediction method should be able to calculate turbulent fuel-air mixing and kinetically controlled combustion in a combustor for arrays of hydrogen injectors at various angles and configurations to the airstream. Other aspects such as the effects of the combustor walls on the flow and the ability to predict the effects of ignition sources are also important. Practical limitations severely restrict the inclusion of all of these capabilities in a single program. In the present work, we consider a simple flow geometry that consists of an axisymmetric diffusion flame of hydrogen in vitiated air. To further simplify the numerical simulation, the supersonic jet is assumed to expand ideally into the coflow stream.

An important concern in supersonic reacting flows is the incomplete combustion due to slow chemical kinetics. There are various approaches in modeling chemical kinetics, namely, frozen flow, complete reaction, equilibrium kinetics, and finite rate kinetics. Frozen flow and complete reaction models represent the two extremes of the modeling. The equilibrium reacting flow approach assumes that the chemical reaction time is much shorter than the time required for mixing and flow residence time. However, in supersonic flows, the gas residence time and chemical reaction time can be comparable. Therefore, the local equilibrium assumption may not be valid for the entire flowfield. This paper is intended to address the problem of finite rate chemistry by simulating the chemical reactions in a free shear layer.

In previous work[1] on axisymmetric supersonic jet flames, the mixing of fuel and oxidant was computed for parallel injection of H_2 into coflowing vitiated air using a two-equation ($k-\epsilon$) turbulence model. The extent of the chemical

reaction was modeled by using three different assumptions: 1) no reaction, 2) complete burning of all fuel mixed with oxygen, and 3) finite rate burning based on the rate of decay of large turbulent eddies into small ones. The last assumption is known as the eddy-breakup (EBU) model. In later work,[2] the numerical model was extended to include the effect of unmixedness.

Recently, Eklund et al.[3] investigated the same flow but with several algebraic eddy viscosity turbulence models. The chemical reaction mechanism included a seven-reaction model involving seven chemical species. However, none of the previous work included the effect of turbulence-chemistry interactions.

For high Reynolds numbers turbulent flows, the interaction between turbulence and chemistry can greatly influence both the mixing and reactive scalar fields in the computation. Although these effects have been studied extensively in the subsonic regime by Janicka and Kollmann,[4] Janicka,[5] Chen,[6] Kollmann and Janicka,[7] and others,[8-10] no comparable studies have been done for supersonic flows. In view of that, we calculate the mean values of the thermochemical variables [i.e., concentrations (mass fractions), temperature, and density] for the scalar field through a probability density function (PDF) approach. An assumed shape for the PDF is used to describe fluctuations in both the mixture fraction and the reaction progress variable.

To account for compressibility effects on the turbulent mixing, which reduce mixing rates between the two streams at supersonic speeds, we have incorporated an empirical correlation that relates the turbulent viscosity to the convective Mach number.

A common practice among the numerical predictions done in the past is that the thermochemical properties are evaluated on the fly when the marching-downstream integration is performed. Such an approach is computationally expensive and becomes undesirable for flows in which the number of chemical species is very large or if more complex turbulence or chemical models are to be tested. A viable alternative used in the present work is a lookup table that contains all of the thermodynamic quantities for all possible states. As a result, the amount of computational time is reduced considerably, but the memory requirements increase due to the table.

This paper consists of four parts. In the first part, the turbulent model is introduced. In addition to the usual set of equations for the velocity field (i.e., $k-\epsilon-g$), an extra governing equation (stagnation enthalpy) is solved so that the mixture enthalpy can be determined from the mixture fraction, stagnation enthalpy, and velocities. Next, the combustion model is discussed, and thermochemical tables are constructed for both chemical models. The equilibrium table has the mixture fraction and the mixture enthalpy as the independent variables, whereas the nonequilibrium table is augmented by the reaction progress variable. The statistical information about the distribution of the thermodynamic states is provided by assuming a certain shape for the joint PDF among the scalars. Finally, the results of the calculations are discussed and compared to measurements in a reacting supersonic axisymmetric jet.

Turbulence Model

The turbulence model is an extension of the widely used $k-\epsilon-g$ combustion model for subsonic flows.[4,11] For supersonic flows, effects of significant levels of kinetic energy must be considered; that is, the mixture enthalpy depends not only on the mixture fraction but also on the Mach number.

The Favre-averaged transport equations for mass, momentum, and energy in a free axisymmetric jet are given by Evans et al.[1] For the energy equation, it is assumed that there is neither radiant energy transfer nor work by body forces. Furthermore, the Soret-Dufour effect is neglected and the unsteady pressure term is not considered. The Lewis number for the laminar and turbulent contributions is taken to be equal to unity so that the energy flux caused by interdiffusion does not appear in this equation. For the momentum equation, only gravity forces are neglected, and the pressure gradient is assumed to be a function of the axial coordinate only. In the present parabolic flows, the static pressure is further assumed to be constant throughout the flowfield and, hence, the pressure gradient is zero. The standard form for the turbulence kinetic energy k and its dissipation rate ϵ in a free shear layer can be found elsewhere.[1,4,10,11]

The corresponding scalar field is described by the mean and variance of the mixture fraction f, which is the normalized mass fraction of an atomic element originating from one of the input streams, usually the fuel stream. The mixture fraction is chosen to be 1 in the fuel stream and 0 in the outer coflowing stream. The transport equations for the mean $\tilde{f}$ and the variance g of the mixture fraction have the following form:

$$\bar{\rho}\tilde{u}\frac{\partial \tilde{f}}{\partial x}+\bar{\rho}\tilde{v}\frac{\partial \tilde{f}}{\partial r}=\frac{1}{r}\frac{\partial}{\partial r}\left[\left(\frac{\mu_l}{Sc}+\frac{\mu_t}{\sigma_f}\right)r\frac{\partial \tilde{f}}{\partial r}\right] \tag{1}$$

$$\bar{\rho}\tilde{u}\frac{\partial g}{\partial x}+\bar{\rho}\tilde{v}\frac{\partial g}{\partial r}=\frac{1}{r}\frac{\partial}{\partial r}\left[\left(\frac{\mu_l}{Sc}+\frac{\mu_t}{\sigma_g}\right)r\frac{\partial g}{\partial r}\right]+2\frac{\mu_t}{\sigma_f}\left(\frac{\partial \tilde{f}}{\partial r}\right)^2-C_g\bar{\rho}\frac{\epsilon}{k}g \tag{2}$$

At Mach numbers above 1, the growth rate of mixing layers and jets is reduced. A correction for the turbulent viscosity similar to that derived by Dash et al.[12] for axisymmetric jets is applied. A factor whose magnitude varies from 1.0 at $M=0.0$–0.2 for large Mach number is multiplied by the turbulent viscosity as computed from the k-ϵ model. The correction factor used by Dash et al.[12] is an empirical expression derived from experimental observations and is formulated as follows:

$$f_{cc}=0.25+0.75/\{1.0+\exp[24.73\ (P-0.2)]\} \tag{3}$$

where the parameter P is $k^{1/2}$ divided by the local speed of sound.

In recent experimental studies,[13,14] it has been observed that the thickness of two-dimensional turbulent shear layers is decreased significantly for Mach numbers larger than the sonic value. The reduction of the shear-layer growth is directly related to a compressible mechanism that occurs between the mixing streams. In order to provide an explanation for such phenomena, Bogdanoff[15] concluded that the convective Mach number could be correlated with the reduction of the shear-layer growth rate. To account for the reduction in turbulent mixing rates due to compressibility effects, an empirical correlation based on Papamoschou's measurements[13] is expressed as a function of the convective Mach number. Therefore, the turbulent viscosity is modified according to the following relationship,

$$\mu_t=\frac{C_D^0\bar{\rho}k^2}{\epsilon}\left\{0.20+\frac{0.80}{1.0+\exp[19.0(M_c^{1.0807}-0.4728)]}\right\} \tag{4}$$

and the convective Mach number is defined as

$$M_c=\frac{M_1(1-\lambda_u)}{(1+\lambda_\rho^{-1/2})\lambda_\gamma^{1/4}} \tag{5}$$

where $\lambda_u=u_2/u_1$, $\lambda_\rho=\rho_2/\rho_1$, $\lambda_\gamma=\gamma_2/\gamma_1$, and $M_1=u_1/a_1$. Subscripts 1 and 2 refer to gases or conditions in the freestreams on the high- and low-speed sides of the shear layer, respectively. The new correlation reduces the mixing rates between two streams at high convective Mach numbers and retains subsonic mixing rates at low convective Mach numbers. Finally, the model constants in the equations for the velocity field are standard values that can be found in the literature.[1,4,10,11,16]

Combustion Model

To describe the chemical reactions in turbulent flows, the conservation equation for individual species needed to be solved. Because of the highly nonlinear nature of chemical reaction rates, time-averaged expansions around mean values produce scores of correlations involving species and temperature, and the expansion may not converge as the temperature and species fluctuations become significant compared to the mean values. Simulation of the effects of turbulence of combustion are primarily through these correlations and neglecting them can severely impair the modeling of turbulent combustion. One common approach for overcoming this problem is to assume an analytical function for the joint PDF among the scalars and to compute the mean chemical source terms by integrating over the allowable domain.[4,5,10,11] In what follows, we will extend this approach to supersonic combustion flows, where two chemical models, one with equilibrium and the other with simplified finite rate chemical kinetics, are considered.

In the equilibrium model, all of the chemical reactions are assumed to be in equilibrium and the thermochemical properties can be determined from the mixture fraction f and the mixture enthalpy h provided that the pressure is given. Although one could solve for the equilibrium compositions by minimizing the Gibbs function when the calculations are carried out, it would require considerable computing time. An alternative approach is to generate a lookup table of thermochemical properties in terms of f and h for all possible conditions. During the calculations, all of the thermochemical quantities can be determined by a multilinear interpolation scheme using the table, avoiding repeated calculations for equilibrium compositions. This approach has been extensively employed for predictions of subsonic turbulent reacting flows,[4-8,11] with significant saving of computing time. However, this computationally efficient scheme is feasible only when the thermochemical states are functions of a small number of scalars.

In the partial equilibrium (or nonequilibrium) model, we assume that the two-body shuffle reactions are equilibrated. Therefore, the progress of chemical reactions is determined entirely by the slow three-body recombination reactions:

$$H + OH + M = H_2O + M \qquad (R1)$$

$$H + O + M = OH + M \qquad (R2)$$

$$H + H + M = H_2 + M \qquad (R1)$$

Through proper combinations of reactive scalars, a single global reaction step can be derived from a detailed reaction mechanism[17,18] that contains the seven essential reaction steps. The progress of this global reaction step can be described by a progress variable q, which has a value of unity when the reactions reach the equilibrium state and a value of zero when there is no reaction at all. With the introduction of an additional reactive scalar, the thermochemical properties are now functions of three scalars: f, h, and q. For turbulent reacting flows, the statistical information about the distribution of the thermodynamic states is needed in order to determine mean values. This information is provided by assuming a certain shape for the joint PDF among the scalars with some parameters to be determined by the moments. For simplicity, the three scalars are assumed to be independent, and a clipped Gaussian distribution[9] is assumed for the mixture fraction, a three-delta function[4,11] for the progress variable, and a single-delta function[4,11] for the mixture enthalpy. Determination of these PDF functions only requires the mean and variance of scalars f, h, and q.

To calculate the mean values of $\tilde{q}$ and its variance p, two more transport equations are necessary. For axisymmetric flows, the parabolic modeled equations are represented as follows,

$$\bar{\rho}\tilde{u}\frac{\partial \tilde{q}}{\partial x} + \bar{\rho}\tilde{v}\frac{\partial \tilde{q}}{\partial r} = \frac{1}{r}\frac{\partial}{\partial r}\left[\left(\frac{\mu_l}{Sc} + \frac{\mu_t}{\sigma_q}\right) r \frac{\partial \tilde{q}}{\partial r}\right] + \frac{1}{2}\bar{\rho}\tau\left(\frac{\epsilon}{k}\right) g\tilde{\chi}_2\tilde{q} + \tilde{S}_q \qquad (6)$$

$$\bar{\rho}\tilde{u}\frac{\partial p}{\partial x} + \bar{\rho}\tilde{v}\frac{\partial p}{\partial r} = \frac{1}{r}\frac{\partial}{\partial r}\left[\left(\frac{\mu_l}{Sc} + \frac{\mu_t}{\sigma_p}\right) r \frac{\partial p}{\partial r}\right] + 2\frac{\mu_t}{\sigma_q}\left(\frac{\partial \tilde{q}}{\partial r}\right)^2 - \bar{\rho}\tau\frac{\epsilon}{k}p(1 - g\tilde{\chi}_2) + 2q''\widetilde{S_q''} \qquad (7)$$

The only new model constants introduced in Eqs. (6) and (7) are the turbulent Prandtl numbers σ_q and σ_p. The parameter τ is the ratio of time scales of velocity and scalar fluctuations. The values assigned to these constants were as follows: $Sc = 1$, $\sigma_q = 0.85$, $\sigma_p = 0.90$, and $\tau = 2.0$.

The equilibrium table for the thermochemical variables at a given $(f - h)$ is calculated with the Chemkin computer code developed by Kee et al.[19] Similarly, the nonequilibrium table for the thermodynamic state of the gas for a given $(f - h - q)$ is also calculated with the Chemkin routines prior to the prediction of the flowfield.

Results and Discussion

In this section, the parabolic code is applied to the prediction of a reacting supersonic axisymmetric jet of hydrogen mixing with vitiated air. Before calculating the jet flow, a nonreacting two-dimensional mixing layer is calculated to validate the compressibility correction to the turbulent viscosity.

Numerical calculations using the empirical correlation, Eq. (4), that relates the turbulent viscosity to the convective Mach number are compared with experimental data[13] for a two-dimensional mixing layer. The shear-layer growth rate normalized by the spreading rate at zero convective Mach number is shown in Fig. 1. In the experiment, the mixing-layer spreading rates are obtained from pitot-pressure surveys for a variety of Mach number-gas combinations. Comparisons between these data and numerical results reveal that the empirical correlation describes reasonably well the spreading rate of nonreactive mixing layers. One can observe from Fig. 1 that the convective Mach number does not have to be very large for compressibility effects to be significant. A second noteworthy feature is that for $M_c > 0.75$ the growth rate appears to approach asymptotically a value roughly 20% of its incompress-

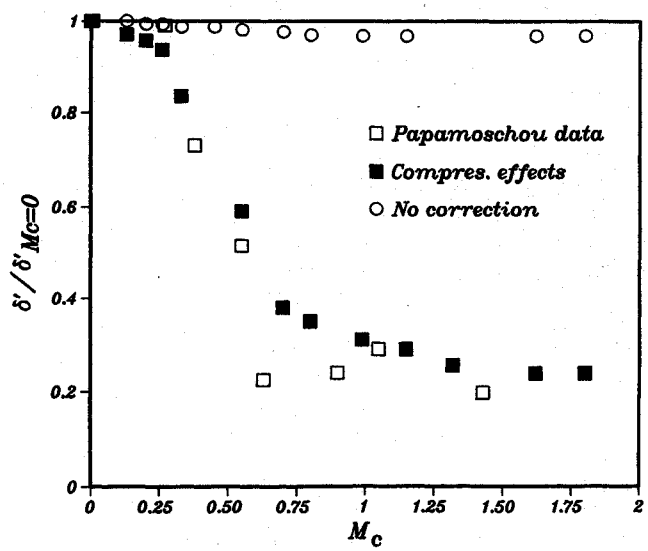

Fig. 1 Comparisons between the numerical results of the present model and experimental data by Papamoschou and Roshko.[13] The shear-layer growth rate normalized by the spreading rate at zero convective Mach number is for a nonreacting two-dimensional mixing layer.

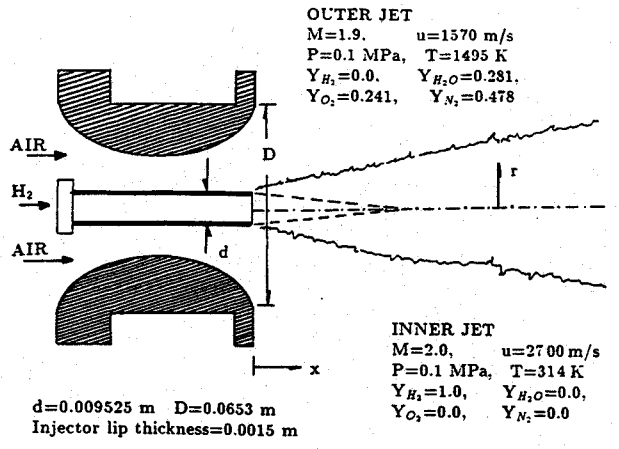

CONVECTIVE MACH NUMBER

$M_1=u_1/a_1=3.245$, $\lambda_u=u_2/u_1=0.557$
$\lambda_\rho=\rho_2/\rho_1=0.4$, $\lambda_\gamma=\gamma_2/\gamma_1=0.892$,

$$M_c=\frac{M_1(1-\lambda_u)}{(1+\lambda_\rho^{-1/2})\lambda_\gamma^{1/4}}=0.55$$

Fig. 2 Inner jet and outer jet inflow conditions for the scale supersonic burner used by Beach reported in Evans et al.[1] The convective Mach number is evaluated at the inflow conditions.

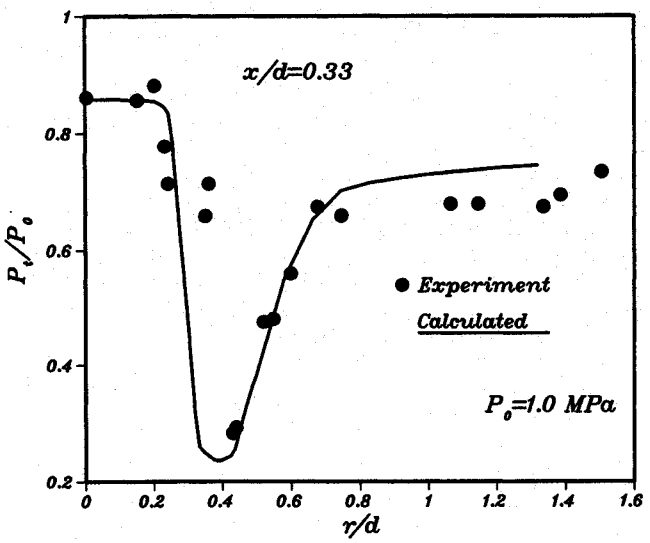

Fig. 3 Initial total pressure profile.

ible value. Also shown in Fig. 1 is the numerical solution corresponding to the normalized spreading rates for the same flow conditions but without the compressibility correction. As expected, the ratio $\delta'/\delta_{M_c=0}$ remains almost constant and very close to 1. This comparison illustrates that the standard $k-\epsilon-g$ turbulence model is inappropriate for supersonic flows.

For reacting supersonic axisymmetric jets, the flow conditions in experiments of Beach reported in Evans et al.[1] are used to evaluate the performance of the parabolic code in axisymmetric reacting flows. A schematic of their coaxial jet flowfield examined in this work is shown in Fig. 2; the temperature and other exit conditions for the nozzle are also given in Fig. 2. To be consistent with the experimental data, the outside diameter (d = 0.009525 m) of the H_2 injector is used to normalize the radial profiles. The present calculations assume that the gases expand ideally into atmospheric air so that shock waves are not present. Furthermore, uniform conditions are used at the inflow boundaries for both the inner and

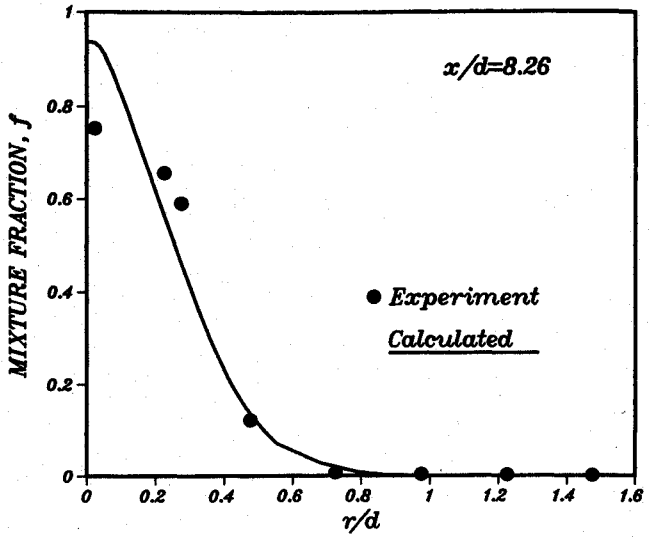

Fig. 4a Radial profile of the predicted and deduced mixture fractions for the nonequilibrium model at x/d = 8.26.

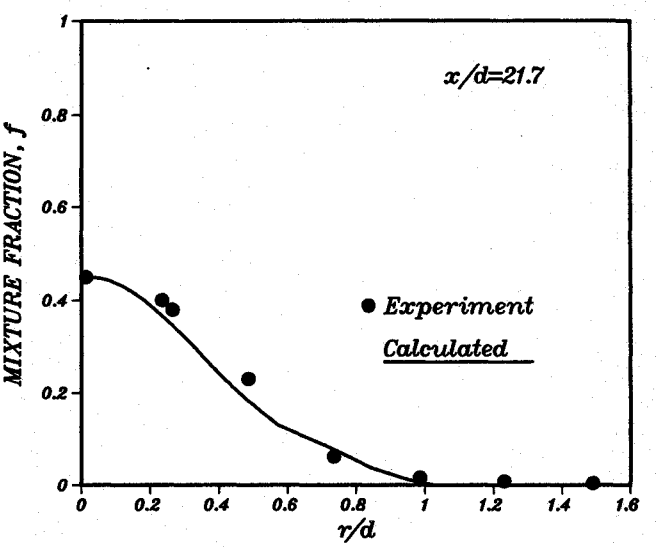

Fig. 4b Radial profile of the predicted and deduced mixture fractions for the nonequilibrium model at x/d = 21.7.

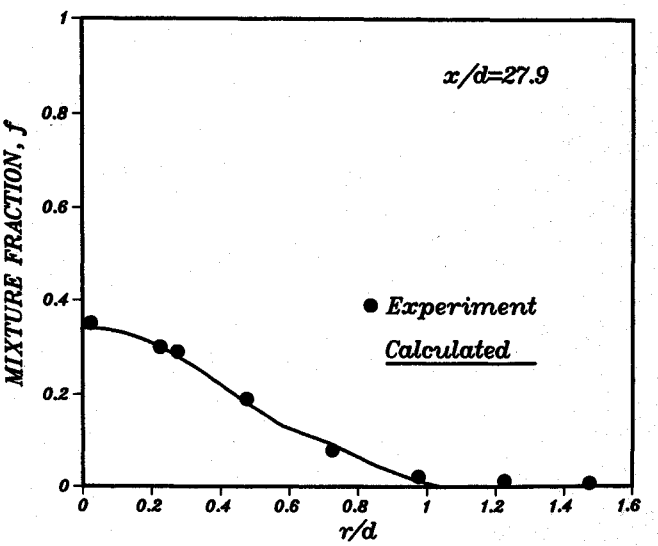

Fig. 4c Radial profile of the predicted and deduced mixture fractions for the nonequilibrium model at x/d = 27.9.

outer jets. The numerical computation for solving the transformed,[20] coupled partial differential equations is carried out by using a block-tridiagonal solver.[21] Fifty grids across half of the jet are used and typically 2000 marching steps are performed. Using a VAX 8650 machine, about 40 min of CPU time are required to calculate the table and approximately 20 min to solve the reacting flow.

The calculations are initiated at $x/d = 0.33$, where the flow measurements were made. The initial velocity profile is computed from the tabulated experimental pitot-pressure data provided by Evans et al.,[1] assuming a constant static pressure of 1 atm. The procedure for calculating the k and ϵ initial profiles is described by Evans et al.[1]

Several test runs were conducted showing that results are sensitive to the initial k and ϵ values. Because of the uncertainty in specifying the initial k and ϵ values, the dissipation length parameter is chosen to achieve good agreement with the experimental data. The value of $l_\epsilon = 0.24$ mm is used for the equilibrium and nonequilibrium models so that the calculated profiles predicted by both chemistry models can be compared. In Fig. 3, the measured total pressure is compared to the initial profile for total pressure used in the present calculations for the nonequilibrium and equilibrium cases. The dip in the profile starting at the inside H_2 injector radius ($r/d = 0.33$) to the outside H_2 injector radius ($r/d = 0.5$) is due to the effect of the thick H_2 injector wall.

One of the most important features of the mixture fraction is that, under the assumption of equal diffusivity, it is independent of the progress of chemical reaction and indicates how well the fuel and oxidizer streams are mixed. To assess the model's capability to predict the mixing process, radial profiles of mixture fraction are plotted at three locations: $x/d = 8.26$, 21.7, and 27.9. A comparison of the experimental data and the numerical predictions is presented in Figs. 4 for the nonequilibrium code. The equilibrium results are similar. Experimental data for the mixture fraction are deduced from the measured mass fractions of the three major species using H as the conserved element

$$f = \frac{Y_{H_2} + (2/18)Y_{H_2O} - (2/18)Y^{\infty}_{H_2O}}{Y^{f}_{H_2} - (2/18)Y^{\infty}_{H_2O}} \tag{8}$$

where superscripts f and ∞ denote the fuel and outer streams at the nozzle exit, respectively. As can be seen from Figs. 4b and 4c, the predictions are in satisfactory agreement with the experimental data, except in Fig. 4a, where the model underpredicts the degree of mixing in the inner part of the jet.

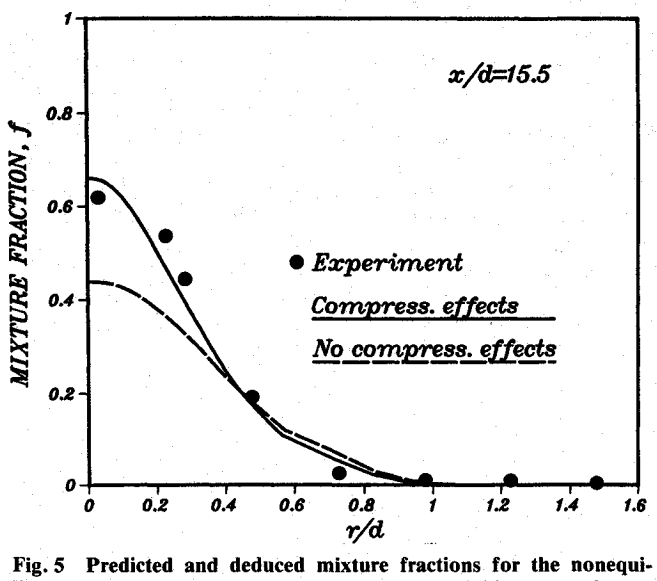

Fig. 5 Predicted and deduced mixture fractions for the nonequilibrium model with and without the compressibility correction at $x/d = 15.5$.

The requirement for the compressibility correction is realized when the mixture fraction profiles with and without the compressibility effects are compared at location $x/d = 15.5$ (see Fig. 5). The disagreement between the two solutions shows that the turbulent mixing rates are incorrectly predicted when the compressibility effects are not present in the turbulence transport model. The compressibility correction to the computed mixture fraction distribution at the far-downstream regions ($x/d > 21.7$) is negligible. This trend is expected since the supersonic spreading rates approach the incompressibility limit as the convective Mach number diminishes downstream.

The calculated profiles of the three minor species at location $x/d = 15.5$ are now examined for the finite rate chemistry and fast chemistry cases. In Fig. 6, the mass fraction distributions of the H, O, and OH radicals are shown for the nonequilibrium model, whereas Fig. 7 shows for the same minor species the profiles with the equilibrium model. For the partial equilibrium model, the concentrations of H, O, and OH and their respective integrated areas are much larger. For kinetically controlled processes, the reaction zone occurs over a much wider domain within the flowfield. In particular, the OH mass fraction distribution has a very tall and sharp peak. Also note that the H mass fraction penetrates much farther into the rich region of the jet than in the equilibrium case.

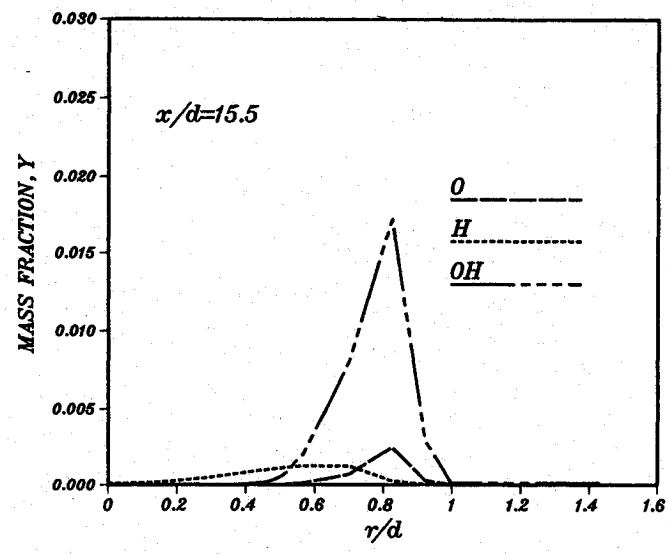

Fig. 6 Radial profiles of the predicted mass fractions of three minor species for the nonequilibrium model at $x/d = 15.5$.

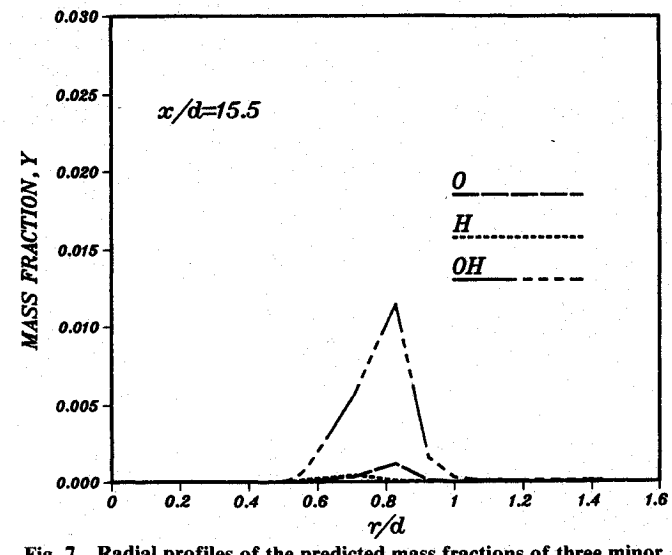

Fig. 7 Radial profiles of the predicted mass fractions of three minor species for the equilibrium model at $x/d = 15.5$.

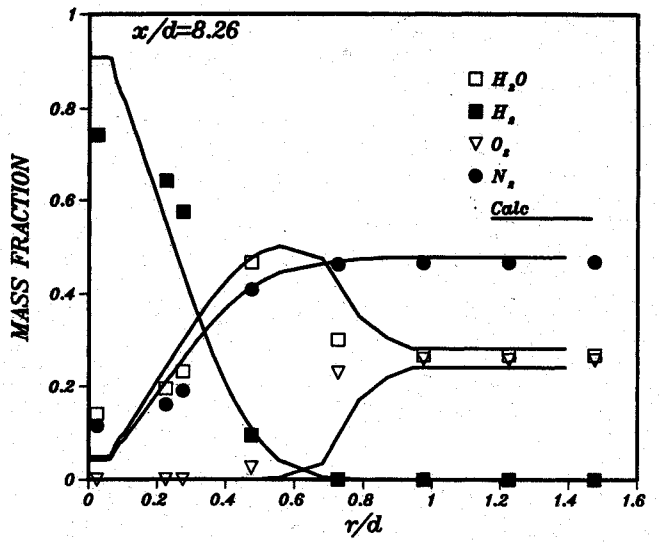

Fig. 8a Radial profiles of the predicted and measured mass fractions of major species for the nonequilibrium model at $x/d = 8.26$.

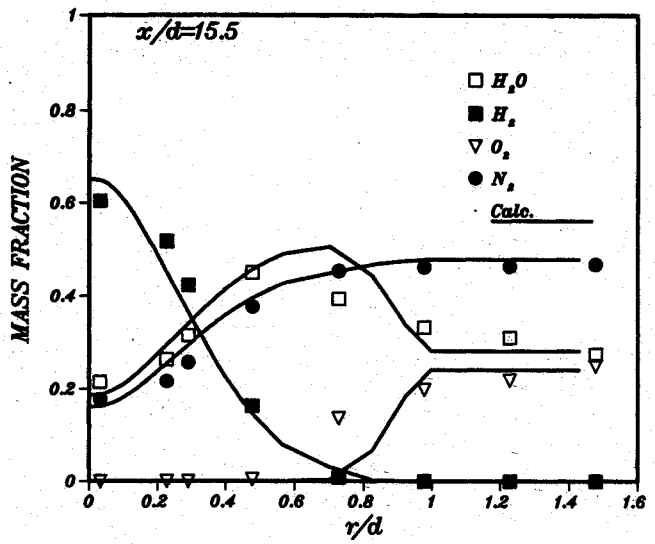

Fig. 8b Radial profiles of the predicted and measured mass fractions of major species for the nonequilibrium model at $x/d = 15.5$.

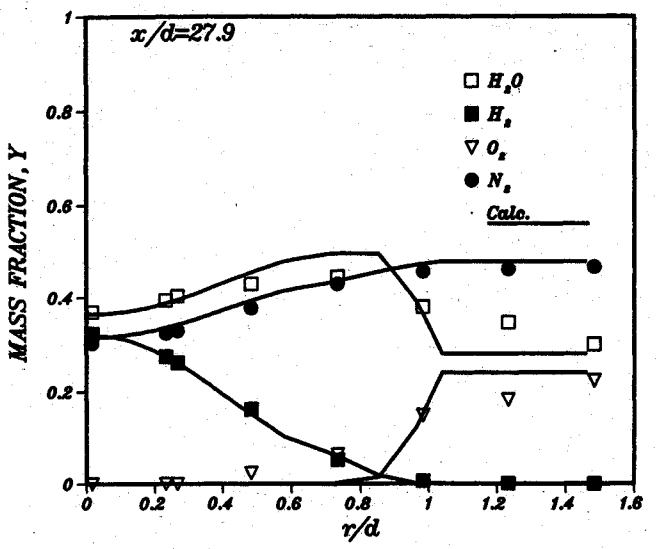

Fig. 8c Radial profiles of the predicted and measured mass fractions of major species for the nonequilibrium model at $x/d = 27.9$.

Referring to Fig. 6, one can see that substantial levels of the H atom mass fraction are produced along the entire radial domain and this is not consistent with the equilibrium results.

The predicted centerline temperatures (not shown) for both chemistry models at $x/d = 8.26$, for example, are about 340 K, and at such temperatures there should be no H atoms ($Y_H^{eq} = 10^{-35}$). However the nonequilibrium model still predicts substantial H atom levels at this position ($Y_H^{noneq} = 1.28 \times 10^{-5}$). Evidently, the partial equilibrium assumption forces bimolecular reactions to proceed even at low temperatures, leading to the unrealistic H atom concentration in the rich cold central cone of the flame. This leads to the conclusion that the partial equilibrium assumption breaks down at low temperatures. Despite the low-temperature restriction, the partial equilibrium assumption works well after the flow is ignited and the reactions are proceeding at temperatures above 1200 K.

All of the comparisons made in this work are well beyond the ignition point of the supersonic flame. This is supported by experimental data previously obtained by Beach[22] on supersonic mixing and combustion in an identical hydrogen jet in a coaxial high-temperature test gas. The apparatus and instrumentation are the same as the one described earlier (see Fig. 2), where supersonic hydrogen (Mach 2) is injected into an unconfined Mach 2 jet of air at 2200 K total temperature. The Mach numbers of the hydrogen jets in both experiments are the same, but the Mach number and stagnation temperature of the vitiated air in our case are 5% smaller and 1.3% larger than those used by Beach.[22] Photographs of the flowfield at test conditions show quite clearly that there is a measurable delay distance before ignition from the hydrogen-air reaction can be seen. This distance is approximately 2.4 diameters (based on the injector outside diameter). This suggests that for $x/d \gg 2.4$ there is ignition, and in our flow, the simplified partial equilibrium model used here is a good approximation to describing the combustion process in this H_2-air supersonic flame.

In general, the concentrations of minor species predicted by the nonequilibrium model are higher than those calculated with the equilibrium model. However, farther downstream ($x/d = 27.9$), both chemistry models predict very closely the same amount of radicals, indicating that an equilibrium state has been reached for the minor species. To evaluate properly the validity of the results of the nonequilibrium model, the minor species need to be measured.

Figures 8a–c compare the predictions and experimental data of the major species concentration distributions for the nonequilibrium model at $x/d = 8.26$, 15.5, and 27.9, respectively. The numerical results match the experimental data well in regions near the H_2 jet, but a fairly substantial difference between the measured and predicted major species mass fraction values is evident at the flame front. The relative position of the peak H_2O concentration reveals that, indeed, O_2 is consumed more rapidly in the calculated results.

Several potential sources of error in the experimental procedure can be identified. Briefly, the mass fractions of H_2, O_2, and N_2 were measured by gas chromatograph. Furthermore, water concentrations are deduced from the dry samples by difference. It is not clear that the gas sampling probes quench the reaction and that the constituents reaching the sample bottle are those present ahead of the probe. As pointed out by Evans et al.,[1] a quantitative indication of the validity of this approach is given by comparison of the measured freestream levels of nitrogen, oxygen, and water vapor as compared with the inflow values for these species. From the reported measured values at freestream and the inflow conditions, one can determine that the error in the measurements ranges from 5 to 15%. For this reason, nonintrusive methods are preferred today, but were not available at the time of the measurements.

The large grid spacing seen in the predicted major species profiles for $r/d > 0.6$ is caused by the rapid expansion of the grid system in the computational domain at the outer jet stream where gradients of the flow variables are considered to be negligible, and less accuracy is required.

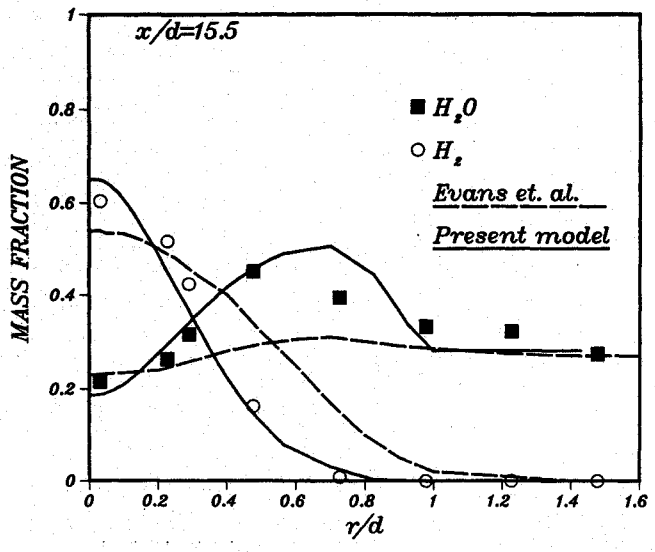

Fig. 9 Numerical predictions of the mass fraction profiles of two major species with the eddy-breakup model and the nonequilibrium model at location $x/d = 15.5$.

Mass fraction profiles of measured and predicted major species for the equilibrium model (not shown) are similar to the nonequilibrium results. Slight differences between the equilibrium and nonequilibrium chemical models are identified mainly in the fuel-rich region where the equilibrium code predicts more H_2 in the centerline. The general agreement is due to the fact that the predictions of stable components and temperature for the partial equilibrium assumption only shows a weak dependence on the progress variable.

It is very profitable to see the improvements of the newly developed nonequilibrium code in contrast to previous predictions of the same flow. Our solution is compared with numerical predictions made by Evans et al.[1] for two reasons. First, their system of transport equations is of parabolic form and, hence, the equations are similar to the ones solved in the present model. Second, their reaction kinetics, in the eddy-breakup model, include only one global reaction ($O_2 + 2H_2 \rightarrow 2H_2O$). The eddy-breakup model is based on the concept of unmixedness, which plays a major role in turbulent flames. The rate constant for the global reaction (C_{EBU}) is not universal and is chosen to achieve the best fit to the data. Evans chooses a single value of C_{EBU} that is valid for the whole flowfield; however, C_{EBU} varies for different flowfields by an order of magnitude (Ref. 1). Figure 9 shows a comparison of numerical predictions of the eddy-breakup model and the nonequilibrium model with measurements for H_2O and H_2 at $x/d = 15.5$. The H_2 distribution predicted by this PDF model is far better than the Evans et al. solution. The Evans et al. solution does not include compressibility effects and overpredicts the rate of mixing.

The use of the eddy-breakup formulation predicts water concentrations that are lower than the experimental measurements. With the use of the PDF model, the agreement is reasonably good, except from $r/d = 0.5$ to 0.9 where greater levels of H_2O are predicted. The partial equilibrium model in superior because it is able to produce H_2O faster in the center of a flame where temperature and concentrations are high and produce more slowly at the edges. A major disadvantage of the eddy-breakup model is that the model has to be adjusted empirically by choice of a constant (C_{EBU}) in the production term of the single global reaction. Little guidance is available as to how to pick this constant.

Conclusions

A numerical model for predicting ideally expanded supersonic turbulent jets with nonpremixed combustion of H_2-air has been developed. Two chemical reaction schemes, one with equilibrium chemistry and the other with a simplified finite rate kinetics, have been incorporated into the present model. The two-equation model adopted for the turbulence model is a modified version of the $k - \epsilon - g$ model tailored for supersonic flows. This program is the first parabolic code to include the turbulence chemistry interaction effects for supersonic flows. A joint PDF describes the interaction between the turbulence and the chemistry due to the turbulent fluctuations of the mixing and reaction scalars. The reduction of the shear-layer growth rate at high speed is quantified by a compressibility correction that is a function of the convective Mach number. The numerical computation is accelerated by the construction of lookup tables that provide all of the instantaneous thermochemical values.

Comparisons of predictions and experimental data by Beach (see Ref. 1) for mixture fraction indicate that the numerical model predicts reasonably well the spreading rates with a modified turbulent diffusion coefficient. Incorporation of the compressibility correction has a strong effect on the turbulence transport process. This correlation makes the parabolic code more robust and versatile, since now it is able to deal with flows in the subsonic and supersonic regimes.

Although the partial equilibrium (PE) model is unable to predict ignition, in the experiment by Beach, ignition occurs early in the flame (2.5 diameters downstream). All of the model/data comparisons of major species are made farther downstream (8 diameters), where the PE model is a good approximation. Only in the cold rich zones (temperatures below 1200 K) does the PE model break down and overpredict the H atom concentrations. Temperature and major species profiles with equilibrium chemistry differ very little from those with the partial equilibrium assumption due to a weak dependence of these variables on the reaction progress variable. The nonequilibrium chemistry model predicts substantially greater concentrations of the minor species.

The use of the thermochemical tables reduces CPU time significantly but increases computer storage. The real benefit of the thermodynamic tables becomes obvious if more complex supersonic flows such as those in a scramjet are studied. A severe limitation of this code is the constant pressure assumption. Thus, it can only be used in those situations in which the inflow pressures at the inner and outer streams are identical or differ by a small amount, say 5%.

Acknowledgments

This work was supported by the U.S. Department of Energy, Office of Basic Energy Sciences, Division of Chemical Sciences, and by National Science Foundation Presidential Young Investigator Grant CTS/8657130. The first author is grateful for the financial support provided by the National Science Foundation and Sandia National Laboratories and the computing facilities provided by Sandia Combustion Research Facility, Livermore, California.

References

[1]Evans, J. S., Schexnayder, C. J., and Beach, H. L., "Application of a Two-Dimensional Parabolic Computer Program to Prediction of Turbulent Reacting Flows," NASA TP-1169, March 1978.

[2]Evans, J. S., and Schexnayder, C. J., "Influence of Chemical Kinetics and Unmixedness on Burning in Supersonic Hydrogen Flames," AIAA Paper 79-0355, Jan. 1979.

[3]Eklund, D. R., Drummond, J. P., and Hassan. H. A., "Calculation of Supersonic Turbulent Reacting Coaxial Jets," *AIAA Journal*, Vol. 28, No. 9, 1990, pp. 1633-1641.

[4]Janicka, J., and Kollmann, W., "A Two-Variable Formalism for the Treatment of Chemical Reactions in Turbulent H_2-Air Diffusion Flames," *Seventeenth Symposium (International) on Combustion*, The Combustion Institute, Pittsburgh, PA, 1979, pp. 412-430.

[5]Janicka, J., "The Application of Partial Equilibrium Assumptions for the Prediction of Diffusion Flames," *Journal of Non-Equilibrium Thermodynamics*, Vol. 6, No. 6, 1981, pp. 367-386.

[6]Chen, J. Y., "Second-Order Conditional Modeling of Turbulent Nonpremixed Flames with a Composite PDF," *Combustion and Flame,* Vol. 69, No. 1, 1987, pp. 1–36.

[7]Kollmann, W., and Janicka, J., "The Probability Density Function of a Passive Scalar in Turbulent Shear Flows," *Physics of Fluids,* Vol. 25, No. 10, 1982, pp. 1755–1769.

[8]Bilger, R. W., "Turbulent Jet Diffusion Flames," *Progress in Energy and Combustion Science,* Vol. 1, No. 1, 1976, pp. 87–109.

[9]Kent, J. H., and Bilger, R. W., "The Prediction of Turbulent Diffusion Flame Fields and Nitric Oxide Formation," *Sixteenth Symposium (International) on Combustion,* The Combustion Inst., Pittsburgh, PA, 1977, pp. 1643–1656.

[10]Jones, W. P., and Whitelaw, J. H., "Calculation Methods for Reacting Turbulent Flows: A Review," *Combustion and Flame,* Vol. 48, No. 1, 1982, pp. 1–26.

[11]Janicka, J., and Kollmann, W., "The Calculation of Mean Radical Concentrations in Turbulent Diffusion Flames," *Combustion and Flame,* Vol. 44, No. 1-3, 1982, pp. 319–336.

[12]Dash, S., Weilersteen, G., and Vaglio-Laurin, R., "Compressibility Effects in Free Turbulent Shear Flows," Air Force Office of Scientific Research, TR-75-1436, Aug. 1975.

[13]Papamoschou, D., and Roshko, A., "The Compressible Turbulent Shear Layer: An Experimental Study," *Journal of Fluid Mechanics,* Vol. 197, 1988, pp. 453–477.

[14]Dimotakis, P. E., "Turbulent Free Shear Layer Mixing," AIAA Paper 89-0262, Jan. 1989.

[15]Bogdanoff, D. W., "Compressibility Effects in Turbulent Shear Layers," *AIAA Journal,* Vol. 21, 1983, pp. 926, 927.

[16]Launder, B. E., and Spalding, D. B., "The Numerical Computation of Turbulent Flows," *Computer Methods in Applied Mechanical Engineering,* Vol. 3, No. 2, 1974, pp. 269–289.

[17]Dixon-Lewis, G., Goldsworthy, F. A., and Greenburg, J. B., "Flame Structure and Flame Reaction Kinetics; IX Calculation of Properties of Multi-Radical Premixed Flames," *Proceedings of the Royal Society of London, Series A: Mathematical and Physical Sciences,* Vol. 346, 1975, pp. 261–278.

[18]Chen, J. Y., "A General Procedure for Constructing Reduced Reaction Mechanisms with Given Independent Relations," *Journal of Combustion Science and Technology,* Vol. 57, No. 1-3, 1988, pp. 89–94.

[19]Kee, R. J., Miller, J. A., and Jefferson, T. H., "CHEMKIN: A General-Purpose Problem-Independent Transportable, Fortran Chemical Kinetics Code Package," Sandia National Lab. Rept. SAND 80-8003, March 1980.

[20]Patankar, S. V., and Spalding. D. B., *Heat and Mass Transfer in Boundary Layers,* 2nd ed., International Textbook, London, 1970.

[21]Chen, J.-Y., Kollmann, W., and Dibble, R. W., "Numerical Computation of Turbulent Free-Shear Flows Using a Block-Tridiagonal Solver for a Staggered Grid System," *Proceedings of the 18th Annual Pittsburgh Conference,* Vol. 18, Instrument Society of America, Pittsburgh, PA, 1987, pp. 1833–1838.

[22]Beach, H. L., "Supersonic Mixing and Combustion of a Hydrogen Jet in a Coaxial High-Temperature Test- Gas," AIAA Paper 72-1179, Nov. 1972.